Proc. of JSCE,
No. 183, Nov. 1970

A METHOD OF ANALYSIS OF WEBPLATES WITH LARGE DEFLECTIONS

*Eiichi Watanabe**
*Ti-Ta Lee***

ABSTRACT

Many attempts have been made to evaluate the buckling loads of plates with various support conditions to predict the strength of plate girders. These attemps have been based on the assumption that the deflections of webplates are relatively small compared with the thickness of the webplates. Due to this assumption, many inappropriate results have been obtained, and the current design practice of plate girders is still based on these results. For this reason, many experimental investigations, and theoretical investigations based on the large deflection theory of plates have been performed.

In this paper, a theoretical method of analysis of webplates with large deflections is proposed. A plate girder panel is simulated by an ideal mechanical model consisting of a thin plate and four beams representing the webplate, two vertical stiffeners, respectively. The loading is a general combination of bending moments and shearing stresses. A method of expanding the unknown displacement components into polynomial series is employed with the magnitude of load taken as the expansion parameter. The sets of linearized partial differential equations are then converted into sets of simultaneous linear algebraic equations by means of finite differences and numerically solved by a digital computer.

I. INTRODUCTION

Unlike columns, the existence of significant strength of plates in their post-buckling range has been known as a fact. The first mathematical formulation was undertaken by von Kármán[1),2)] to account for the effect of large deflection of plates. Škaloud and Donea[3)] investigated the effect of residual stresses on the post-buckling behavior of plates, in which it was indicated that the residual stresses may sometimes result in a real prestressing effect in shear panels. Stein[4),5)] employed a method similar to a perturbation method in his analysis of simply supported initially flat plates subjected to longitudinal compression and to a uniform temperature rise, respectively. Mansfield made use of a method similar to Stein's in his analysis of a compressed square plate[6),7)].

On the other hand, an extensive experimental investigation on welded plate girders was undertaken by Basler and the others[8),9),10),11)]. As a result, the concepts of load carrying capacity were established. In a panel subjected to bending moment, some portion of webplate in the compression zone is assumed to offer no resistence to the bending moment; whereas, in a shear panel, a diagonal

* Ph.D., Assistant Prof., Dept. of Civil Engr., Kyoto Univ.
** Ph.D., Associate Prof., Dept. of Civil Engr., Iowa State Univ.

tension field is assumed in such a way that the flanges do not provide the anchor to this tension field.

The purpose of this study is to analyze the behavior of rectangular plate girder panels subjected to the load beyond their buckling load, and to investigate the significance of the buckling load in reference to their ultimate load. The specific interests of the study include the effects of the initial deflection of web-plates, the residual stresses, the rigidities of boundary members, and the yield strength of steel.

II. PROPOSED ANALYSIS

Fig. 1 shows a plate girder panel system consisting of a rectangular web-plate, two flanges and two vertical stiffeners. This panel system is assumed to remain linearly elastic until the yielding initiates.

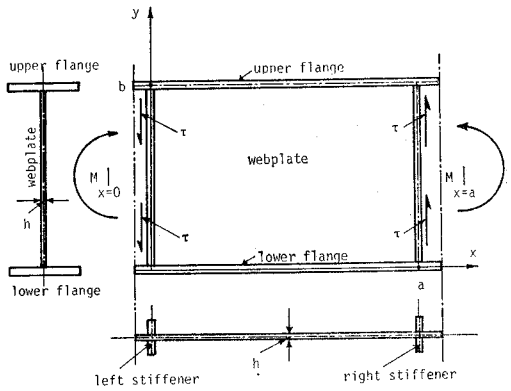

Fig. 1 Plate girder panel

The proposed analysis requires solution of the displacement components $u(x, y)$, $v(x, y)$ and $w(x, y)$ in x-, y-, and z-directions, respectively. The kinematic indeterminacy of the system is six, of which three refer to the displacement components $u(x, y)$ and $v(x, y)$; while the other three refer to the displacement components $w(x, y)$. To eliminate the rigid body motion, it is assumed for convenience that

$$\left.\begin{aligned} &u(0, 0)=u(0, b)=0\,, \\ &v(0, 0)=0\,, \\ &w(0, 0)=w(0, b)=w(a, 0)=0\,. \end{aligned}\right\} \tag{2.1}$$

The torsional buckling of the compression flange and the lateral buckling of beam are not explicitly considered in this paper. Then, the flexural rigidities of the boundary members about their strong axes are so large that it can be assumed that

$$w_{,ss}(x, y)=0\,^{*} \quad \text{along all boundaries,} \tag{2.2}$$

where the subscript s refers to a length measured along the boundaries.

Similarly, due to the existence of the adjacent panels, the flexural rigidities of stiffeners about their weak axes are so large that it can be assumed that

$$u_{,yy}(x, y)=0\,^{*} \quad \text{along edges } x=0 \text{ and } x=a\,. \tag{2.3}$$

Then, it follows from Eqs. (2.1), (2.2) and (2.3) that

---

* Throughout this paper, $(\,)_{,z}$ and $(\,)_{,zz}$ refer to the first and second partial derivatives of certain function with respect to a variable z, respectively, unless otherwise referred to.

$$\left.\begin{aligned} &u(0, y)=0, \quad \text{and} \\ &w(x, y)=0 \quad \text{along all boundaries.} \end{aligned}\right\} \tag{2.4}$$

Consequently, the girder panel shown in Fig. 1 can be idealized and represented by a mechanical model shown in Fig. 2.

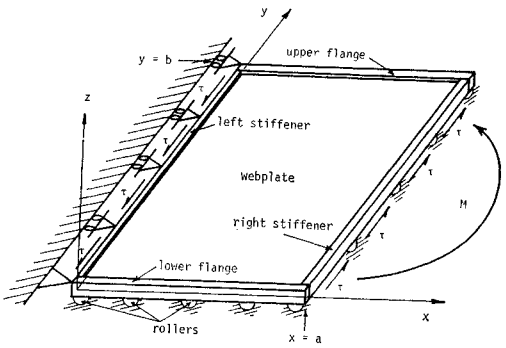

Fig. 2 Idealized model of a plate girder panel.

The displacement can be represented by a vector with components u, v and w. Let w, w_0, $w^{(0)}$ and w^* designate the deflection due to load, initial total deflection, initial elastic deflection and initial inelastic deflection, respectively, then the total deflection, w^T, is obtained by the following equation:

$$w^T=w_0+w=w^*+w^{(0)}+w\,. \tag{2.5}$$

On the other hand, it is assumed that the initial in-plane displacement components u_0 and v_0 are zero; hence

$$u^T=u \quad \text{and} \quad v^T=v\,. \tag{2.6}$$

Using the Lagrangean coordinate system assuming that $w\gg u$ and v, the components of the total strain as applied to thin plates with large deflection can be expressed as follows:

$$\begin{pmatrix} \bar{\varepsilon}_x^T & \varepsilon_{bx}^T \\ \bar{\varepsilon}_y^T & \varepsilon_{by}^T \\ \bar{\gamma}_{xy}^T & \gamma_{bxy}^T \end{pmatrix} = \begin{pmatrix} \bar{\varepsilon}_x & \varepsilon_{bx} \\ \bar{\varepsilon}_y & \varepsilon_{by} \\ \bar{\gamma}_{xy} & \gamma_{bxy} \end{pmatrix} + \begin{pmatrix} \varepsilon_{x0} & \varepsilon_{bx0} \\ \varepsilon_{y0} & \varepsilon_{by0} \\ \gamma_{xy0} & \gamma_{bxy0} \end{pmatrix}, \tag{2.7}$$

$$(\varepsilon_{x0}, \varepsilon_{y0}, \gamma_{xy0})=\frac{1}{2}(w_{0,x}^2, w_{0,y}^2, 2w_{0,x}w_{0,y})\,,$$

$$\begin{pmatrix} \bar{\varepsilon}_x & \varepsilon_{bx}^T \\ \bar{\varepsilon}_y & \varepsilon_{by}^T \\ \bar{\gamma}_{xy} & \gamma_{bxy}^T \end{pmatrix} = \begin{pmatrix} D_x & 0 & w_{0,x}D_x \\ 0 & D_y & w_{0,y}D_y \\ D_y & D_x & w_{0,x}D_y+w_{0,y}D_x \end{pmatrix} \begin{pmatrix} u & 0 \\ v & 0 \\ w & 0 \end{pmatrix}$$

$$-z\begin{pmatrix} 0 & D_{xx} \\ 0 & D_{yy} \\ 0 & 2D_{xy} \end{pmatrix} w_e^T+\frac{1}{2}\begin{pmatrix} w_{,x}^2 & 0 \\ w_{,y}^2 & 0 \\ 2w_{,x}w_{,y} & 0 \end{pmatrix}, \quad \text{and}$$

$$w_e^T=w^{(0)}+w\text{: Total elastic deflection,}$$

where D_x, D_y, D_{xx}, D_{xy}, D_{yy} are linear differential operators; for instance,

$$D_x\equiv\frac{\partial}{\partial x}\,, \quad D_y\equiv\frac{\partial}{\partial y}\,, \quad D_{xy}\equiv\frac{\partial^2}{\partial x\partial y} \quad \text{and} \quad D_{xx}\equiv\frac{\partial^2}{\partial x^2}\,.$$

According to the Hooke's law, the stress-strain relationship is given by the following equations:

$$\begin{bmatrix} \bar{\sigma}_x & \sigma_{bx} \\ \bar{\sigma}_y & \tau_{by} \\ \bar{\tau}_{xy} & \tau_{bxy} \end{bmatrix} = E \begin{bmatrix} \frac{1}{1-\nu^2} & \frac{\nu}{1-\nu^2} & 0 \\ \frac{\nu}{1-\nu^2} & \frac{1}{1-\nu^2} & 0 \\ 0 & 0 & \frac{1}{2(1+\nu)} \end{bmatrix} \begin{bmatrix} \bar{\varepsilon}_x & \varepsilon_{bx} \\ \bar{\varepsilon}_y & \varepsilon_{by} \\ \bar{\gamma}_{xy} & \gamma_{bxy} \end{bmatrix}. \tag{2.8}$$

where subscript b refers to the plate bending.

Substitution of Eq. (2.7) into Eq. (2.8) results in the stress-displacement relationships.

Among several yield criteria, von Mises yield criterion is generally accepted for steel; hence, this is used in predicting the initiation of yielding in this study.

If lateral loads are absent, the following equations of equilibrium are obtained in the domain of the webplate:

$$\left.\begin{aligned} &\bar{\sigma}_{x'x}^T + \bar{\tau}_{xy'y}^T = 0\,, \\ &\bar{\tau}_{xy'x}^T + \bar{\sigma}_{y'y}^T = 0\,, \\ &\nabla^4 w_e{}^T = \frac{h}{D}(\bar{\sigma}_x{}^T D_{xx} + \bar{\sigma}_y{}^T D_{yy} + 2\bar{\tau}_{xy}^T D_{xy}) w^T\,, \end{aligned}\right\} \tag{2.9}$$

where D=flexural rigidity of plate, and
h =thickness of plate.

Substitutions of Eqs. (2.7) and (2.8) into Eq. (2.9) result in the following equations of equilibrium:

$$\begin{bmatrix} D_x & 0 & D_y \\ 0 & D_y & D_x \\ w_{,xx}^T & w_{,yy}^T & 2w_{,xy}^T \end{bmatrix} \left\{ \begin{bmatrix} \frac{1}{1-\nu^2} & \frac{\nu}{1-\nu^2} & 0 \\ \frac{\nu}{1-\nu^2} & \frac{1}{1-\nu^2} & 0 \\ 0 & 0 & \frac{1}{2(1+\nu)} \end{bmatrix} \left\{ \begin{bmatrix} D_x & 0 & w_{0,x}D_x \\ 0 & D_y & w_{0,y}D_y \\ D_y & D_x & w_{0,x}D_y + w_{0,y}D_x \end{bmatrix} \begin{bmatrix} u \\ v \\ w \end{bmatrix} + \frac{1}{2} \begin{bmatrix} w_{,x}^2 \\ w_{,y}^2 \\ 2w_{,x}w_{,y} \end{bmatrix} \right\} + \frac{1}{E} \begin{bmatrix} \sigma_{x0} \\ \sigma_{y0} \\ \tau_{xy0} \end{bmatrix} \right\} - \frac{D}{Eh} \begin{bmatrix} 0 \\ 0 \\ \nabla^4 \end{bmatrix} w_e{}^T = \begin{bmatrix} 0 \\ 0 \\ 0 \end{bmatrix}. \tag{2.10}$$

Kirchhoff established two basic relationships for the interaction of the plate element and an adjacent boundary member element. One relates the torsion of the plate element to the bending of the boundary member element; while another relates the bending of the plate element to the torsion of the boundary element. From the mechanical model considered here, only the latter needs to be considered. For instance, the boundary conditions along $x=0$ are given as follows:

$$w_e{}^T=0 \quad \text{and} \quad \{(GJ_s+EI_0v_{,y})D_{xyy}-D(D_{xx}+\nu D_{yy})\}w_e{}^T=0\,, \tag{2.11}$$

where GJ_s and I_0 refer to the torsional rigidity and the polar moment of inertia of the left stiffener, respectively.

In general, two relationships can be obtained to designate the interaction of the plate element with an adjacent boundary element. One refers to the longitudinal equilibrium of the boundary element, and the other refers to the transverse equilibrium of the same element. For instance, letting σ_f' denote the axial stress in the compression flange,

$$\sigma_{f',x}'+\frac{h}{A_f'}\bar{\tau}_{xy}^T=0\,, \quad \text{and} \quad (EI_f'D_{xxxx}-A_f'\sigma_f'D_{xx}+h\bar{\tau}_{xy}^TD_x)v=h\bar{\sigma}_y{}^T \quad \text{along} \quad y=0\,, \tag{2.12}$$

and letting σ_s' denote the axial stress in the right stiffener,

$$\sigma_{s',x}'+\frac{h}{A_s'}\bar{\tau}_{xy}^T=-\frac{h}{A_s'}\tau \quad \text{and} \quad u_{,yy}=0 \quad \text{along} \quad x=a\,, \tag{2.13}$$

where EI_f' refers to the flexural rigidity of the lower flange about its weak axis, and A_f', A_s' refer to the cross sectional areas of the tension flange, the right stiffener, respectively.

Since no in-plane compressive loads act perpendicular to a boundary member, the corresponding resultant force should vanish along the boundary. For instance, along $x=0$:

$$h\int_0^b \bar{\sigma}_x{}^T\,dy\,\Big|_{x=0}+A_f\sigma_f\,\Big|_{x=0}+A_f'\sigma_f'\,\Big|_{x=0}=0\,. \tag{2.14}$$

The bending moment along $x=a$ should be of a uniquely assigned value; whereas, there exist no external bending moments acting along $y=0$ and $y=b$. For instance, along $x=a$:

$$h\int_0^b \bar{\sigma}_x{}^T y\,dy\,\Big|_{x=a}-bA_f\sigma_f\,\Big|_{x=a}=M\,\Big|_{x=a}\,. \tag{2.15}$$

Previous experimental results have shown that the most common initial deflectional pattern is of one half wave in both x- and y-directions. Furthermore, flanges and stiffeners can be considered not to deform significantly before loads are applied. Thus, the following initial deflectional surface is assumed in this paper:

$$w_0(x,y)=A\left(1-\cos\frac{2\pi x}{a}\right)\left(1-\cos\frac{2\pi y}{b}\right). \tag{2.16}$$

Fig. 3 shows a typical residual in-plane stress distribution in a plate girder with flanges continuously welded along the edges of the webplate[12),13)]. If vertical stiffeners are weld-

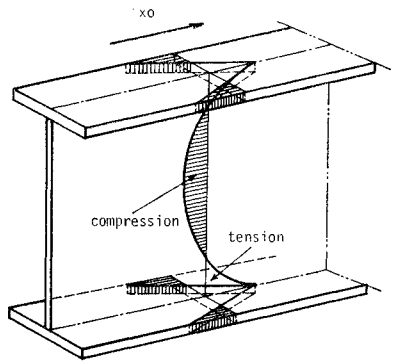

Fig. 3 Typical residual stress distribution caused by continuous longitudinal welding.

ed furthermore, the residual stress distribution is affected. The residual stress used herein is mainly based on the one used in References 3. The residual stress components are assumed in the following form:

$$\left.\begin{aligned}\sigma_{x0}&=-\frac{1}{2}\sigma_0\left(\frac{a}{b}\right)^2\left\{1-4\left(\frac{x'}{a}\right)^2\right\}^2\left\{1-12\left(\frac{y'}{b}\right)^2\right\},\\ \sigma_{y0}&=-\frac{1}{2}\sigma_0\left\{1-12\left(\frac{x'}{a}\right)^2\right\}\left\{1-4\left(\frac{y'}{b}\right)^2\right\}^2,\\ \tau_{xy0}&=-8\sigma_0\frac{x'y'}{b^2}\left\{1-4\left(\frac{x'}{a}\right)^2\right\}\left\{1-4\left(\frac{y'}{b}\right)^2\right\},\end{aligned}\right\} \tag{2.17}$$

where

$$x'=x-\frac{1}{2}a \quad \text{and} \quad y'=y-\frac{1}{2}b, \quad \text{and} \quad \sigma_0\equiv\sigma_{y0}\Big|_{\substack{x'=a/2\\ y'=0}}.$$

Fig. 4 shows typical load-displacement curves of webplates with initial deflections subjected to in-plane loads[14),15)]. An observation that the displacement components may be well expressed in polynomial series throughout the loading process with first, second and third powers in terms of the magnitude of load suggests the following forms of solutions:

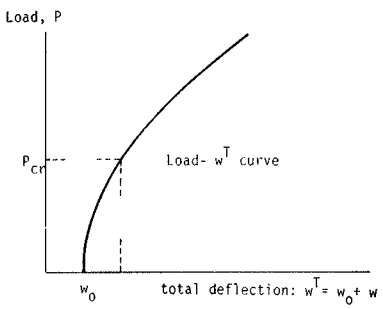

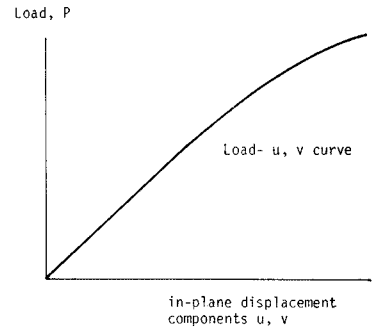

Fig. 4 Typical load-displacement curves.

$$\left.\begin{aligned}u(x,y)&=\sum_{k=0}^{\infty}u^{(k)}(x,y)\Delta^k,\\ v(x,y)&=\sum_{k=0}^{\infty}v^{(k)}(x,y)\Delta^k, \quad \text{and}\\ w(x,y)&=\sum_{k=0}^{\infty}w^{(k)}(x,y)\Delta^k.\end{aligned}\right\} \tag{2.18}$$

Substitutions of Eq. (2.18) into the equations of equilibrium, Eq. (2.10), and the boundary conditions using the stress-displacement relationships result in several sets of linearized partial differential equations expressed in terms of polynomial series of Δ. The terms corresponding to the first power may be identified as those which can be considered in the usual small deflection theory of plates. The terms corresponding to the second power will be found to introduce the first approximation to the large deflection of plates. Solutions of additional higher power will give the second and then higher approximations. In this paper, consideration will be limited only up to the third power because of great complexity involved in the solution process for the powers higher than the third. Besides, it must be kept in mind that the consideration of higher power terms does not guarantee greater accuracy.

Fig. 5 illustrates a load-deflection curve approximated segmentwise. This curve is seen divided into several intervals*. Let points $P_1, P_2, \cdots, P_n$ designate the partition points of the curve into intervals $I_1, I_2, \cdots, I_n$. Also, let $\Delta_1, \Delta_2, \cdots, \Delta_n$ designate the loads corresponding to points $P_1, P_2, \cdots, P_n$. Then, the procedure of solving the given problem can be summarized as follows:

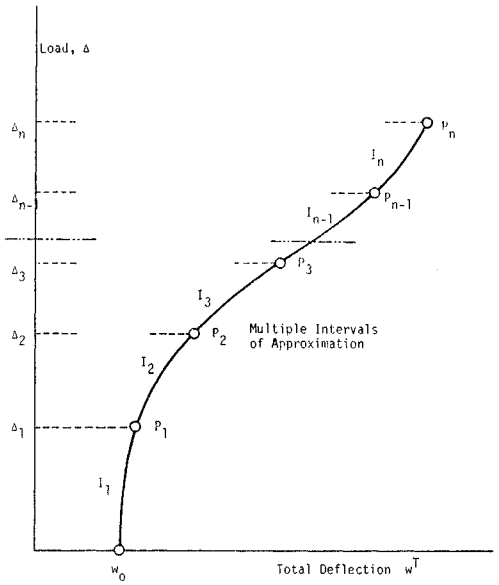

Fig. 5 Segmentwise approximation of the load-deflection curve.

In the first interval, I_1:

1. Solve the zero order equation to find $w^{(0)}$, then evaluate the zero order bending stress components, σ_{bx0}, σ_{by0} and τ_{bxy0},

2. Solve the first order equations to find $u^{(1)}$, $v^{(1)}$ and $w^{(1)}$, then evaluate the stress components such as $\bar{\sigma}_x^{(1)}$, $\bar{\sigma}_y^{(1)}$, $\sigma_{bx}^{(1)}$ and $\tau_{bxy0}^{(1)}$,

3. Solve the second order equations to find $u^{(2)}$, $v^{(2)}$ and $w^{(2)}$, then evaluate the stress components such as $\bar{\sigma}_x^{(2)}$, $\bar{\tau}_{xy}^{(2)}$ and $\sigma_{by}^{(2)}$,

4. Solve the third order equations to fine $u^{(3)}$, $v^{(3)}$ and $w^{(3)}$, then evaluate the third order stress components,

5. Obtain the total displacements u^T, v^T and w^T, and the total stress components $\bar{\sigma}_x{}^T$, $\bar{\sigma}_y{}^T$, $\bar{\tau}_{xy}^T$, σ_{bx}^T, σ_{by}^T, τ_{bxy}^T by substituting the value of load level, Δ, each time evaluating von Mises yield comparison stresses and principal stresses,

6. Set $u_0=u^T$, $v_0=v^T$ and $w_0=w^T$, $\sigma_{x0}=\bar{\sigma}_x{}^T$, $\sigma_{y0}=\bar{\sigma}_y{}^T$, $\tau_{xy0}=\bar{\tau}_{xy}^T$, and $\sigma_{bx0}=\sigma_{bx}^T$, $\sigma_{by0}=\sigma_{by}^T$, and $\tau_{bxy0}=\tau_{bxy}^T$ at $\Delta=\Delta_1$.

In intervals $I_2, I_3, \cdots, I_n$:

7. Repeat the procedures 2 through 6 where in each new interval, the load parameter is newly defined by $\tilde{\varepsilon}:\tilde{\varepsilon}=\Delta-\Delta_{j-1}$ in interval I_j, in which $\tilde{\varepsilon}$ is a small positive number such that $0\leqq\tilde{\varepsilon}<\min(|w^{(1)}|/|w^{(2)}|)$. Repeat this procedure until the terminal point P_n is reached.

In the average edge shearing stress, τ, is taken as the load parameter, then, Δ, its nondimensionalized form, can be conveniently defined by the following expression:

$$\Delta=\frac{\tau}{\sigma_{Yw}}, \tag{2.19}$$

where σ_{Yw} refers to the yield strength of webplate. This expansion parameter is also used in the case of combined bending and shear.

If the externally applied bending moment, M, is taken as the load parameter, then, Δ, its nondimensionalized form, can be conveniently defined by the following expression:

---

* Let these intervals be called multiple intervals of approximation.

$$\Delta=\frac{M}{\sigma_{Yw}ha^2}\,. \tag{2.20}$$

If bending moment and shearing force act simultaneously, the following parameter is used to designate the interaction between them:

$$\theta=\frac{bM\,|_{x=a}}{\tau ba^2}\,. \tag{2.21}$$

III. NUMERICAL SOLUTIONS BY MEANS OF FINITE DIFFERENCES

It is extremely difficult to solve the problem analytically mainly because the boundary conditions are quite sophisticated. For this reason, each set of linearized equations are numerically solved by the use of finite difference method. The mechanical model illustrated in Fig. 2 is converted into sets of discrete points as shown in Figs. 6(a) through 6(c). In these figures, N designates the size of mesh point system, or the number of mesh lines in one direction inside the domain of the webplate. It is to be noted that three unknowns, namely, $u(x, y)$, $v(x, y)$ and $w(x, y)$ correspond to one grid point. It is seen that the total number of unknowns on this $N\times N$ mesh point system is

$$3N^2+7N-7\,.$$

The computer programs used herein consist of a main program and 12 subroutine subprograms. A set of simultaneous algebraic equations are repeatedly solved for each order of approximation by a library subroutine subprogram based on the Gaussian Elimination Method.

The input parameters to the computer programs consist of the following:

1. index, designating the type of loading, namely, either shear, bending or the combination of the two,

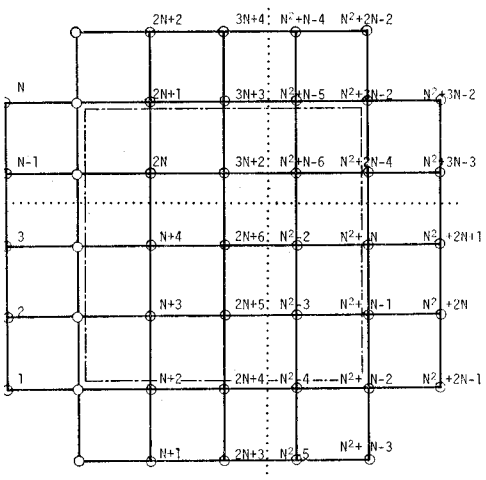

Fig. 6(a) Generalized mesh point system for $u(x, y)$.

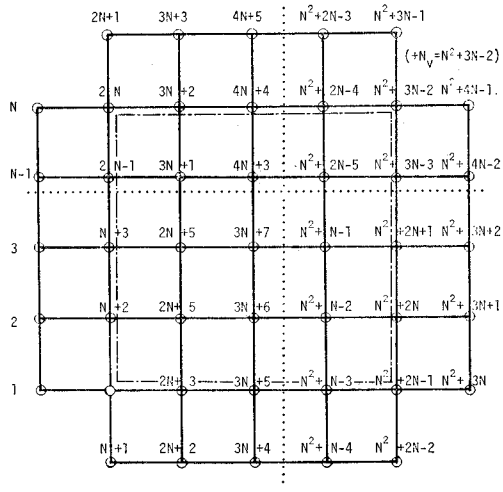

Fig. 6(b) Generalized mesh point system for $v(x, y)$.

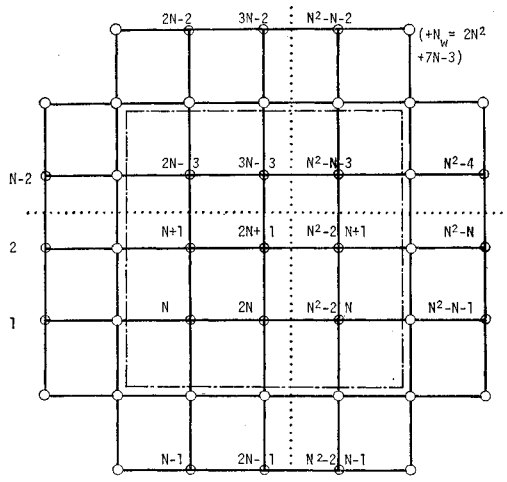

Fig. 6(c) Generalized mesh point system for $w(x, y)$.

2. aspect ratio of panel: $\lambda=b/a$,
3. slenderness ratio of webplate: $\beta=a/h$,
4. parameters designating the cross sectional areas of
   upper and lower flanges, ϕ_f and ϕ_f', respectively, and
   left and right stiffeners, ϕ_s and ϕ_s', respectively,
5. parameters designating the torsional rigidities of
   upper and lower flanges, ψ_f and ψ_f', respectively, and
   left and right stiffeners, ψ_s and ψ_s', respectively,
6. flexural rigidity parameters of the upper and lower flanges about their weak axes, κ_f and κ_f', respectively,

where the rigidity parameters of boundary member m, for instance, are defined by the following expressions:

$$\phi_m=\frac{A_m}{ah},\quad \psi_m=24(1-\nu)\frac{J_m}{h^3a}\quad\text{and}\quad \kappa_m=64(1-\nu^2)\frac{1}{\beta^2}\frac{i_m}{h^3a}, \tag{2.22}$$

in which A_m, J_m and i_m refer to the cross sectional area, torsional rigidity constant and the moment of inertia about the weak axis, of boundary member m, respectively.

7. ratio of the magnitude of the maximum residual stress to the Modulus of Elasticity of steel: $\alpha=\sigma_0/E$,
8. ratio of the magnitude of the maximum residual stress to the yield strength of steel: $\zeta=\sigma_0/\sigma_{Yw}$,
9. ratio of the magnitude of the maximum initial deflection to the thickness of webplate: $\mu=A/h$,
10. bending-shear interaction parameter, θ.

IV. NUMERICAL ILLUSTRATION AND DISCUSSIONS ON THE ANALYTICAL RESULTS

To verify the proposed analysis, several test results are cited[16),17),18)]. They are analyzed and compared with the results from the proposed analysis. Tests reported in References 16 and 17 will be referred to as Lehigh tests; while those reported in Reference 18 will be referred to as Japanese tests. Twelve tests are cited from Lehigh tests and three are cited from Japanese test. Various parameters in the test girders are provided in Table 1.

Past experiments have shown that the load carrying capacity of a deep bending panel is most frequently governed by the vertical buckling of flange, lateral buckling of girder and the torsional buckling of the compression flange rather than by the yielding of the webplate.

Table 1 Calculation of parameters in test girders

Test Girder No.	Type of Load	λ = b/a	β = a/h	ϕ_f	ϕ_f'	ϕ_s	ϕ_s'	ψ_f	ψ_f'	ψ_s	ψ_s'	κ_f 10^{-4}	κ_f' 10^{-4}	μ_{ex}	Δ_{wcr}	Δ_u^{ex}
G1-T1	M	0.667	278	0.43	0.46	0.10	0.10	6.1	6.1	0.47	0.47	0.7	2.3	0.139	0.21	0.242
G2-T1	M	0.667	278	0.46	0.47	0.10	0.10	21.0	21.6	0.47	0.47	2.4	2.4	0.157	0.21	0.378
G3-T1 *	M	0.724	278	0.42	0.46	0.10	0.10	168.4	21.1	0.48	0.48	320.0	2.0	0.148	0.24	0.381
G4-T1	M	0.667	582	0.97	0.98	0.21	0.21	195.2	189.0	4.35	4.35	5.0	5.0	0.407	0.07	0.563
G5-T1 *	M	0.724	581	1.14	0.97	0.21	0.21	1536.0	191.9	4.34	4.34	669.0	4.2	0.833	0.08	0.495
G6-T1	S	0.667	389	0.65	0.65	0.14	0.14	59.4	59.4	1.30	1.30	3.4	3.4	0.376	0.08	0.328
G7-T1	S	1.000	255	0.96	0.95	0.20	0.20	79.0	81.6	1.86	1.86	11.0	10.9	0.446	0.11	0.389
G8-T1	C	0.333	761	0.31	0.30	0.47	0.47	25.0	24.4	23.30	23.30	0.4	0.4	0.355	0.11	0.226
G9-T1	C	0.333	1145	0.46	0.46	0.71	0.71	85.6	82.6	78.90	78.90	0.6	0.6	0.286	0.04	0.165
F10-T1	C	0.667	292	0.83	0.83	0.31	0.08	69.9	70.0	6.59	0.67	7.1	7.1	0.108	0.12	0.342
F10-T2	S	0.667	292	0.83	0.83	0.08	0.08	69.9	70.0	0.67	0.67	7.1	7.1	0.157	0.16	0.371
F10-T3	S	0.833	234	1.04	0.04	0.10	0.10	87.4	87.4	0.83	0.83	20.0	20.0	0.053	0.19	0.382
A-M	M	1.000	267	0.53	0.53	0.40	0.40	21.3	21.3	8.95	8.95	2.6	2.6	0.167	0.22	0.640
B-Q	S	1.000	267	0.53	0.53	0.40	0.40	21.3	21.3	8.95	8.95	2.6	2.6	0.167	0.10	0.282
C-M	M	1.000	200	0.40	0.40	0.30	0.30	9.0	9.0	3.78	3.78	2.0	2.0	0.125	0.19	0.555

* circular tubed compression flange

The analysis of a bending panel by the proposed analysis, therefore, consists of checking these bucklings from the solutions obtained. The procedure to evaluate the strength of the panel is summarized as follows:

1. evaluation of the flange stresses using the solved displacement components $u(x, y)$ along the flanges.
2. investigation of the yielding of the webplate using von Mises yield criterion,
3. investigation of the possibility of the vertical buckling of the flange,
4. investigation of the possibility of the lateral buckling of girder,
5. investigation of the possibility of torsional buckling of the compression flange.

The buckling criteria used herein are essentially those presented in Reference 8; however, they are omitted in this paper.

In this paper, computations are restricted to the single interval of approximation for simplicity. The results of the behavioral analysis are demonstrated by Figs. 7 through 12.

Fig. 7 shows a load-σ_f relationship of test girder G1-T1, where σ_f refers to the average compressive stress in the compression flange at the point concerned. This relationship shows that it is approximately linear. Furthermore, it is found not significantly affected by the magnitude of initial deflection of webplate.

Fig. 8 shows a load-$\bar{\sigma}_x$ relationship of test girder G1-T1. In this particular case, several computer results with different initial stresses and initial deflections all coincide approximately with the experimental values.

Fig. 9 shows a deflectional surface of the webplate in test girder A-M computed from the proposed analysis. This figure shows a general trend that the deflection of webplate in the compression zone is more pronounced than that in the tension zone. The figure shows that the deflectional surface is basically symmetric with respect to $x=a/2$, and has some skew symmetry. This small skew symmetry comes from the third power term while the symmetry comes from the second power term of solutions $w(x, y)$. This skew symmetry could have resulted from the small differences of boundary conditions at $x=0$ and $x=a$, or from the cumulative error associated with the finite differences. The ex-

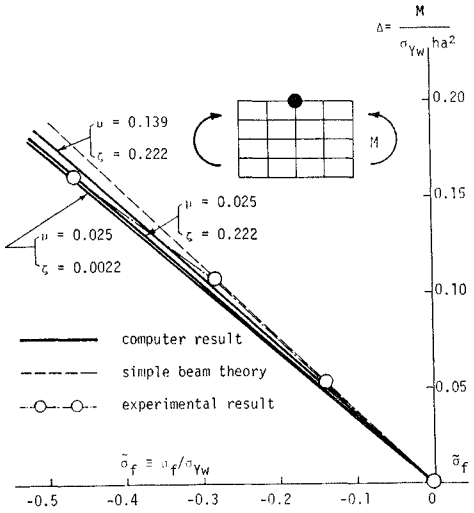

Fig. 7 Load-σ_f curve: Test girder G1-T1.

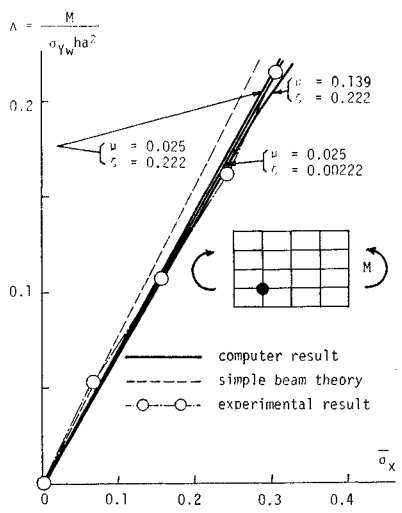

Fig. 8 Load-$\bar{\sigma}_x$ curve: Test girder G1-T1.

perimental deflectional surface was by no means symmetric. Although the proposed analysis fails to predict the solutions above the yielding load, $\Delta^{th}_{\max}$, rough estimation of the ultimate load, Δ^{th}_{ult}, may be obtained by an extrapolation formula: $\Delta^{th}_{\text{ult}} \simeq \Delta^{th}_{\max} \times \sigma_{\text{cr}}/\sigma_{\text{fav}}$. It was mentioned earlier that consideration was limited to the single interval of approximation in this paper; however, Δ^{th}_{ult} will be directly obtained if the multiple intervals of approximation are employed. Various values of initial deflection and initial in-plane stresses are assumed for the theoretical computation since it is found through the investigation that the initial in-plane stresses are the least known parameters among many parameters among many parameters considered. The accuracy of the measurements of initial deflections, first of all, may be questioned. Besides, the initial in-plane stresses were not actually measured in any of the tests cited. Except for those, the prediction of the ultimate loads will be found quite satisfactory.

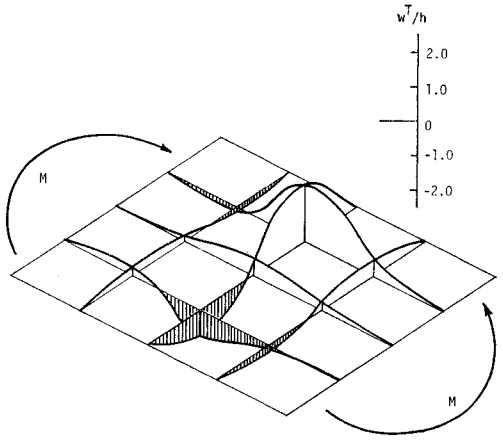

Fig. 9 Deflectional surface of webplate: Test girder A-M: μ=0.025; ζ=0.005; Δ=0.65.

Fig. 10 shows an in-plane displacement configuration of test girder A-M. It is seen that the upper flange undergoes compression and the lower flange undergoes elongation.

Fig. 11 shows the distribution of $\bar{\sigma}_x$ across the depth of girder panel A-M obtained from the proposed analysis. It is seen that the compressive stress is much reduced compared with the tensile stress in the webplate.

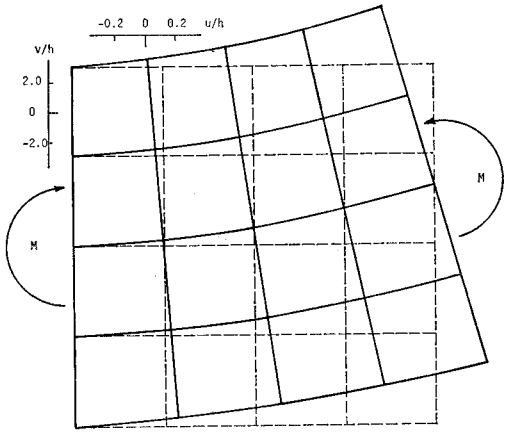

Fig. 10 In-plane displacement configuration: Test girder A-M: μ= 0.025; ζ=0.005; Δ=0.65.

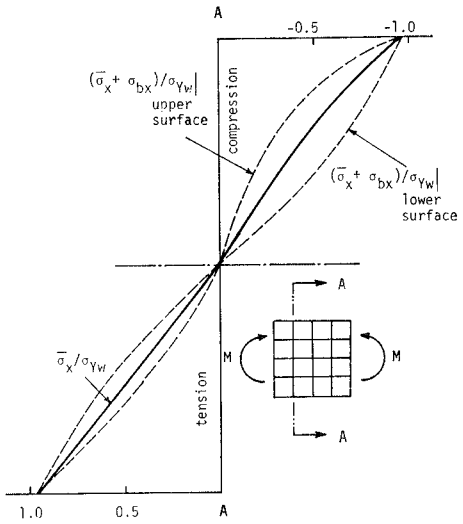

Fig. 11 Distribution of $\bar{\sigma}_x$ across the depth of girder: Test girder A-M: μ=0.025; ζ=0.005; Δ= 0.65.

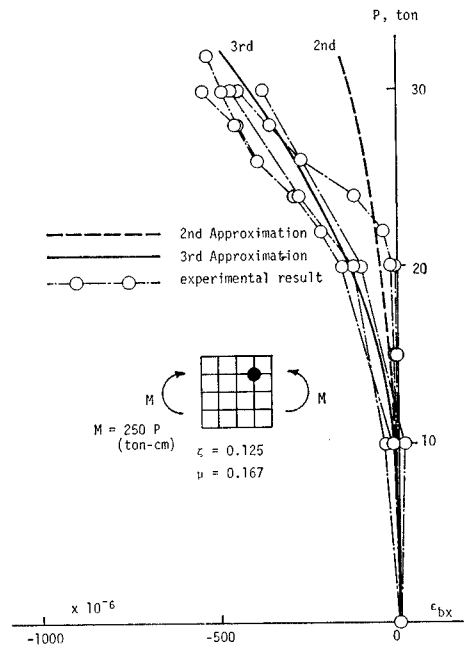

Fig. 12 P-ε_{bx} relationship: Test girder A-M: 2nd and 3rd order approximations.

Fig. 12 shows a load-ε_{bx} relationship of test girder A-M, where ε_{bx} designates a bending strain component. In this figure, both the 2nd and 3rd order approximations are shown for comparison with the test results. It may be seen that the third order approximation is in better agreement with the experimental results. The experimental strains plotted were obtained from the total strain components ε_{bx}^{T} by eliminating the residual strain components.

Many experiments have shown that the ultimate load of a shear panel is always governed by the yielding along the diagonal line. This yielding is caused by a significantly large stress in the direction of the diagonal line. This phenomenon is ordinarily referred to as a diagonal tension field and is characterized by an outstanding bulge along the diagonal line.

The analysis of computed results based on the proposed theoretical analysis consists of checking the deflectional surfaces, yielding of the diagonal line, and load-σ_1, σ_2 relationships, where σ_1 and σ_2 designate the maximum and minimum principal stresses, respectively. The ultimate load of a shear panel is found by finding the load at which interior points on the diagonal line initiate yielding.

Basler's theory is also applied for comparison with the ultimate strength evaluated by the proposed analysis. Furthermore, overall behavior of a shear panel as predicted by the proposed analysis is compared with simple pure shear case and with experimental results whenever available. The simple pure shear refers to the case of an ideal flat plate subjected to pure shear condition. Results of this analysis is demonstrated by Figs. 13 through 15.

Fig. 13 shows a load-σ_1, σ_2 relationship of test girder B-Q. This figure shows a general trend that the maximum principal stress tends to increase rapidly with the load, while the minimum principal stress tends to creep with the load. This trends is found very prominent when the magnitude of the initial deflection is large.

Fig. 14 shows a deflectional surface of test girder B-Q. This figure shows outstanding bulge in the direction of the diagonal line of the webplate; furthermore, the deflectional surface is of typical three half waves peculiar to the shear problem.

Fig. 15 shows an in-plane displacement configuration in test girder B-Q. The panel is seen to deform into a parallelogramic shape.

The results of computations are shown in Tables 2, 3 and 4. In these tables, the ultimate loads of the test girders are predicted using 5×5 mesh point system and the single interval of approximation of the load-displacement curves. In Table 2,

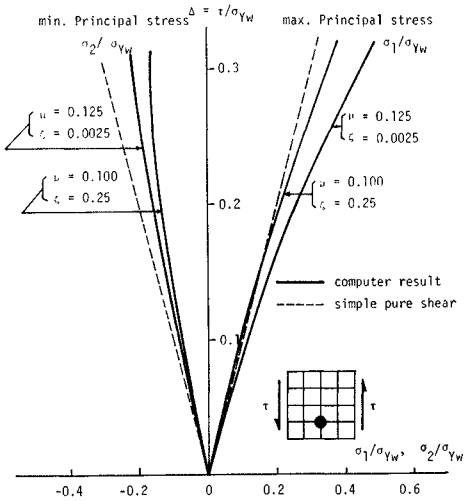

Fig. 13 Load-σ_1, σ_2 curves: Test girder B-Q.

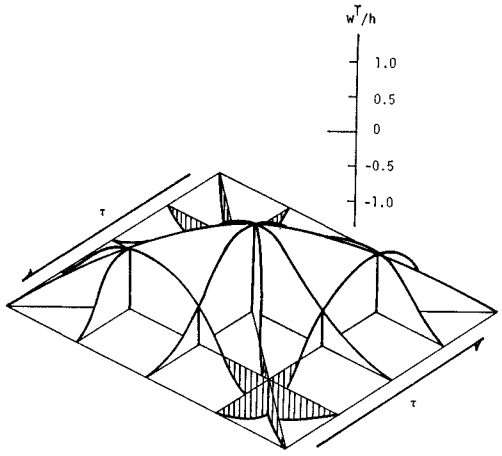

Fig. 14 Deflectional surface of webplate: Test girder B-Q: $\mu=0.125$; $\zeta=0.0025$; $\Delta=0.28$.

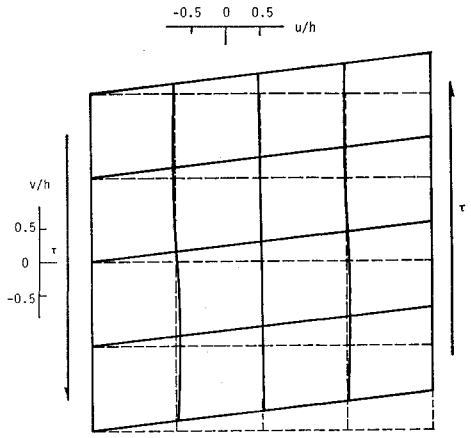

Fig. 15 In-plane displacement configuration: Test girder B-Q: $\mu=0.025$; $\zeta=0.25$; $\Delta=0.32$; $\theta=-0.5$.

Table 2 Prediction of ultimate load for bending panels

Girder No.	Δ_{ult}^{ex}	Δ_{wcr}	Mode of Fail.[a]	μ_{ex}	$\left(\frac{\sigma_r}{\sigma_{Yw}}\right)_{th}$[b]	μ_{th}	$\frac{\sigma_{cr}}{\sigma_{fav}}$	Δ_{max}^{th}	Δ_{ult}^{th}	Δ_{ult}^{B}[c]
G1-T1	0.242	0.21	T.B.	0.139	0.005	0.025	1.00	0.21	0.21	0.22
					0.500	0.025	1.09	0.18	0.20	0.22
					0.500	0.139	1.21	0.18	0.22	0.22
G2-T1	0.378	0.21	L.B.	0.157	0.005	0.025	1.13	0.35	0.40	0.39
					0.500	0.025	1.80	0.20	0.36	0.39
					0.005	0.125	1.17	0.36	0.42	0.39
					0.500	0.157	1.94	0.20	0.39	0.39
					0.005	0.157	1.29	0.33	0.42	0.39
G3-T1	0.381	0.24	L.B.	0.148	0.005	0.025	1.08	0.39	0.42	0.37
G4-T1	0.563	0.07	L.B.	0.407	0.005	0.025	1.02	0.60	0.61	0.56
					0.005	0.125	1.50	0.39	0.59	0.56
G5-T1	0.495	0.08	L.B.	0.833	0.005	0.025	1.26	0.54	0.68	0.48
					0.005	0.100	1.57	0.42	0.66	0.48
A-M	0.640	0.22	T.B.	0.167	0.005	0.025	1.06	0.65	0.69	0.63
					0.125	0.025	1.09	0.64	0.70	0.63
					0.500	0.125	1.74	0.42	0.73	0.63
					0.500	0.025	1.54	0.45	0.69	0.63
					0.001	0.167	1.17	0.56	0.66	0.63
					0.125	0.167	1.74	0.36	0.63	0.63
C-M	0.555	0.19	T.B.	0.125	0.003	0.025	1.03	0.54	0.56	0.46
					0.150	0.125	1.52	0.33	0.50	0.46
					0.003	0.125	1.03	0.48	0.49	0.46

[a] T.B. = Torsional Buckling and L.B. = Lateral Buckling.

[b] σ_r refers to the maximum residual stress and is given by:

$\sigma_r = \sigma_0$ for $\lambda \geq 1$ and $\sigma_r = \sigma_0/\lambda^2$ for $\lambda \leq 1$.

[c] Ultimate load obtained by Basler's theory.

Table 3 Prediction of ultimate load for shear panels

Girder	Δ_{ult}^{ex}	Δ_{wcr}	μ_{ex}	σ_r/σ_{Yw}	μ_{th}	Δ_{ult}^{th}	Δ_{ult}^{B}	θ_{ex}	θ_{used}
G6-T1	0.328	0.077	0.376	0.005	0.125	0.26	0.317	-0.667	-0.667
				0.005	0.100	0.26	0.317	-0.667	-0.667
G7-T1	0.389	0.105	0.446	0.500	0.025	0.44	0.395	-1.500	-1.500
				0.500	0.025	0.45	0.395	-1.500	-0.500
				0.005	0.100	0.36	0.395	-1.500	-0.500
				0.005	0.125	0.32	0.395	-1.500	-0.500
F10-T2	0.371	0.159	0.157	0.005	0.125	0.38	0.364	0.214	0.214
				0.005	0.125	0.40	0.364	0.214	-0.500
				0.500	0.125	0.40	0.364	0.214	0.214
F10-T3	0.382	0.185	0.053	0.005	0.125	0.40	0.407	0.400	0.400
				0.005	0.100	0.42	0.407	0.400	0.400
				0.500	0.053	0.34	0.407	0.400	0.400
B-Q	0.282	0.022	0.167	0.250	0.025	0.30	0.338	-1.167	-1.167
				0.003	0.025	0.38	0.338	-1.167	-1.167
				0.003	0.125	0.24	0.338	-1.167	-1.167
				0.250	0.167	0.12	0.338	-1.167	-0.500
				0.250	0.050	0.32	0.338	-1.167	-0.500
				0.003	0.025	0.38	0.338	-1.167	-0.500
				0.003	0.125	0.28	0.338	-1.167	-0.500

Table 4 Prediction of ultimate load for panels subjected to bending and shear combined

Girder	Δ_{ult}^{ex}	Δ_{wcr}	μ_{ex}	σ_r/σ_{Yw}	μ_{th}	Δ_{ult}^{th}	θ	Actual Failure
G8-T1	0.226	0.110	0.355	0.005	0.125	0.30	0.000	Diagonal Tension
				0.005	0.200	0.24	0.000	
				0.500	0.025	0.34	0.000	
G9-T1	0.165	0.040	0.286	0.005	0.125	0.20	0.000	Diagonal Tension
				0.005	0.150	0.18	0.000	
F10-T1	0.342	0.120	0.108	0.005	0.125	0.32	0.747	Diagonal Tension
				0.500	0.125	0.26	0.747	
				0.500	0.108	0.26	0.747	

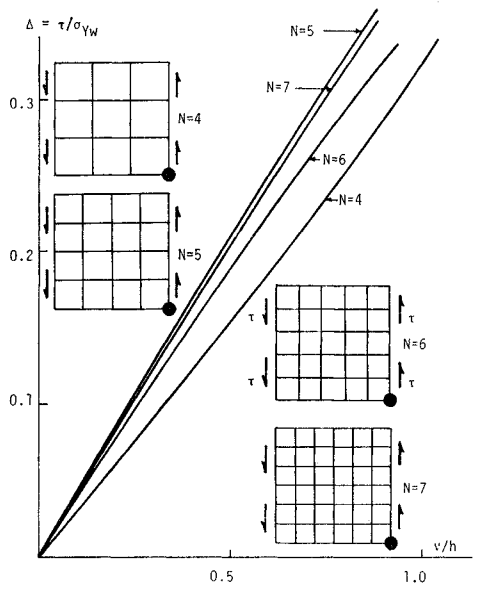

Fig. 16 Load-v curve: Convergence check: Due to shear load, τ.

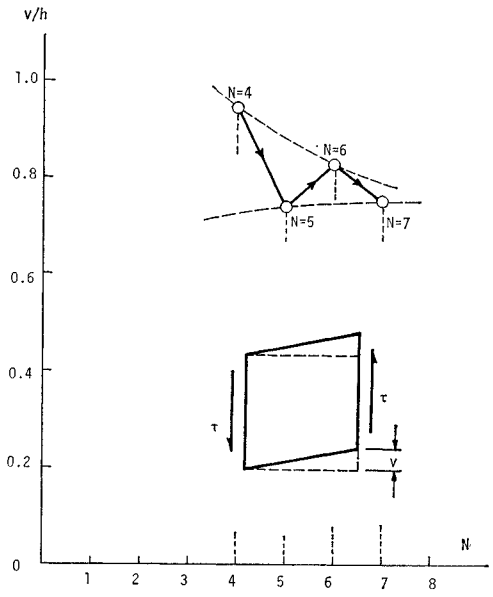

Fig. 17 Convergence curve for v: Test girder B-Q: Δ=0.30.

$\Delta^{th}_{\max}$ corresponds to the magnitude of load at which the yielding initiates in the panel system. On the other hand, σ_{fav} and σ_{cr} refer to the average stress in the compression flange and the minimum of the torsional, and lateral buckling load, respectively.

Figs. 16 and 17 show some of the convergence curves for test girder B-Q. These figures show a good convergence of 5×5 mesh point system. Similar results were obtained for bending panels.

V. CONCLUSIONS

The proposed analysis is based on the expansion of the displacement components in terms of the load parameter. In this paper, computations are made using single interval of approximation, and the results can be summarized as follows:

1. The contribution of the 3rd power terms in the in-plane displacement components u and v is usually less than 10% of the total of the 1st through the 3rd power terms,

2. The contribution of the 3rd power terms in the deflection w can be sometimes as high as 30% of the total deflection, w^T. Besides, the 2nd power term of w is usually the greatest for webplates with relatively long post-buckling range and zero power term is the greatest for webplates with large initial deflection and relatively short range of post-buckling,

3. The contribution of the 3rd power terms in the in-plane stress components is usually small, namely, less than 5% of the total of the zero through the 3rd power terms. Furthermore, the 1st power terms are usually greater than the 2nd and the 3rd power terms,

4. The contribution of the 3rd power terms in the plate bending stress components is approximately in the same order of those corresponding to the 1st and 2nd power terms,

5. Larger initial deflection causes more curved load-displacement and load-stress relationships,

6. Larger initial deflection causes larger deflection in the webplate. The in-plane displacement components, however, are not significantly affected by the initial deflection,

7. The pattern of the initial deflection does not necessarily cause a similar deflectional shape of webplate due the loading,

8. Larger boundary rigidity leads, in general, to more stable behavior of girder panels in the post-buckling range. However, excessive reinforcement of the boundary members does not prove to be beneficial in the case of shear panels,

9. The larger the yield strength of steel is, the larger the post-buckling strength of the panel becomes,

10. The proposed analysis can take into account several bucklings by removing the rollers supporting edge $y=b$ and using appropriate boundary conditions, and by using the multiple intervals of approximation of the load-displacement component curves. This modification is being undertaken by one of the authors.

ACKNOWLEDGEMENT

This study was sponsored by the Engineering Research Institute of Iowa State University, Ames, Iowa, U.S.A. The numerical computations were performed by the University Computer, IBM System 360 Model 65.

BIBLIOGRAPHIES

1) von Kármán, T., "Festigkeitsprobleme im Maschinenbau," *Encyklopädie der Mathematischen Wissenschaften*, Vol. 4, No. 4, 1910, p. 311.
2) von Kármán, T., Sechler, E. E. and Donnell, L. H., "The Strength of Thin Plates in Compression," *Transactions*, ASME, Vol. 54, No. 2, 1932, p. 53.
3) Škaloud, M. and Donea, J., "Post-critical Behavior of Webs with Residual Stresses," IABSE, *Publications*, Vol. 23, 1963, p. 293.
4) Stein, M., "Behavior of Buckled Rectangular Plates," *Journal of Engineering Mechanics Division*, ASCE, Vol. 86, No. EM2, 1960, p. 59.
5) Stein, M., "Loads and Deformations of Buckled Rectangular Plates," *Technical Report*, NASA, No. R40, 1959.
6) Mansfield, E. H., "The Bending and Stretching of Plates," International Series of Monographs on Aeronautics, Pergamon Press Ltd., Oxford, 1964.
7) Mansfield, E. H., "Some Identities on Structural Flexibility after Buckling," *Aeronautical Quarterly*, Vol. 9, 1958, p. 300.
8) Basler, K. and Thurlimann, B., "Strength of Plate Girders in Bending," *Journal of Structural Division*, ASCE, Vol. 87, No. ST6, 1961, p. 153.
9) Basler, K., "Strength of Plate Girders in Shear," *Journal of Structural Division*, ASCE, Vol. 87, No. ST7, 1961, p. 151.
10) Basler, K., "Strength of Plate Girders under Combined Bending and Shear," *Journal of Structural Division*, ASCE, Vol. 87, No. ST7, 1961, p. 181.
11) Gaylord, E. H., "Discussion for Strength of Plate Girders in Shear," *Journal of Struc-*

tural Division, ASCE, Vol. 88, No. ST2, 1962, p. 151.
12) Beedle, L. S., Blackman, J. H., Cooper, P. B., Driscoll, G. C., Jr. and Eney, W. J., "Structural Steel Design," Ronald Press Inc., New York, N. Y., 1964.
13) Rao, N. R. N. and Tall, L., "Residual Stresses in Welded Plates," Fritz Engineering Laboratory, Department of Civil Engineering, Lehigh University, *Fritz Engineering Laboratory Report*, No. 249.7, 1960.
14) Rockey, K. C. and Jenkins, F., "The Behavior of Webplates of Plate Girders Subjected to Pure Bending," *The Structural Engineer*, Vol. XXXV, No. 5, 1957, p. 176.
15) Mueller, J. A. and Yen, B. T., "Girder Web Boundary Stresses and Fatigue," Welding Research Council, *Bulletin*, Vol. 127, 1968.
16) Basler, K., Yen B. T., Mueller, J. A. and Thurlimann, B., "Web Buckling Tests on Welded Plate Girders," *Bulletin Series*, Welding Research Council, Vol. 64, 1960.
17) Patterson, P. J., Corrado, J. A., Huang, J. S. and Yen, B. T., "Proof-tests of Two Slender-web Welded Plate Girders," Fritz Engineering Laboratory, Department of Civil Engineering, Lehigh University, *Fritz Engineering Laboratory Report*, No. 327.7, 1969.
18) "Theories and Experiments of the Load Carrying Capacity of Plate Girders (translated)," Kansai Research Committee on Bridges, Steel Frames and Welding, Nippon Publishing Company, Inc., Osaka, 1965.

(*Received April 15, 1970*)